

Two inequivalent sublattices and orbital ordering in MnV_2O_4 studied by ^{51}V NMR

S.-H. Baek,¹ N. J. Curro,² K.-Y. Choi,³ A. P. Reyes,⁴ P. L. Kuhns,⁴ H. D. Zhou,⁴ and C. R. Wiebe⁴

¹*Los Alamos National Laboratory, Los Alamos, New Mexico 87545, USA*

²*Department of Physics, University of California, Davis, California 95616, USA*

³*Department of Physics, Chung-Ang University, Seoul 156-756, Republic of Korea*

⁴*National High Magnetic Field Laboratory, Tallahassee, Florida 32310, USA*

(Received 25 August 2009; published 9 October 2009)

We report detailed ^{51}V NMR spectra in a single crystal of MnV_2O_4 . The vanadium spectrum reveals two peaks in the orbitally ordered state, which arise from different internal hyperfine fields at two different V sublattices. These internal fields evolve smoothly with externally applied field, and show no change in structure that would suggest a change of the orbital ordering. The result is consistent with the orbital ordering model recently proposed by Sarkar *et al.* [Phys. Rev. Lett. **102**, 216405 (2009)] in which the same orbital that is a mixture of t_{2g} orbitals rotates by about 45° alternately within and between orbital chains in the $I4_1/a$ tetragonal space group.

DOI: 10.1103/PhysRevB.80.140406

PACS number(s): 75.25.+z, 76.60.-k, 75.10.-b, 75.50.Gg

Competition between spin interactions and orbital degeneracy is a key factor in determining the ground-state magnetic and lattice structure of transition-metal oxides and gives rise to a rich spectrum of phase transitions in magnetic insulators.^{1,2} Recently, vanadium oxide spinels of the form AV_2O_4 have attracted interest in which A is a divalent transition element that is either nonmagnetic^{3–5} (Mg, Zn, and Cd) or magnetic^{6–10} (Mn). The intriguing physics of the vanadate compounds arises from the geometrical spin frustration of the triply degenerate t_{2g} orbitals of V^{3+} ($3d^2, S=1$) in the spinel structure. The V ions sit at the vertices of corner-sharing tetrahedra, and experience a magnetic exchange interaction with nearest-neighbor V spins. In the process of relieving spin frustration, the vanadates typically undergo two consecutive phase transitions. First, a structural distortion splits the t_{2g} levels into a low-lying xy orbital and a higher doublet (yz, zx) at a temperature T_S . This structural phase transition is accompanied by long-range orbital ordering of the V orbitals since Hund's rules imply that a single electron occupies the excited doublet and orbital exchange interactions lift this degeneracy. If the A site is nonmagnetic, then the V spins order antiferromagnetically at a lower temperature $T_N < T_S$.

When the A site is magnetic, features emerge that are distinct from the other vanadates. In particular, for $\text{Mn}^{2+}(3d^5)$ a ferrimagnetic (FEM) transition occurs *before* the structural transition ($T_S < T_N$). The combination of strong ferromagnetic Mn-Mn couplings, antiferromagnetic (AFM) Mn-V couplings, and AFM V-V couplings leads to a collinear FEM spin configuration at $T_N \sim 56$ K. This collinear state retains the orbital degeneracy but is unstable so that upon further cooling the V spins become noncollinear below the structural transition at $T_S = 53$ K. Once again, long-range orbital order of the V d orbitals emerges in concert with structural distortion. However, the nature of the orbital symmetry remains poorly understood and continues to be debated theoretically in the literature.^{11–14} Experimentally, Adachi *et al.* proposed the ferro-orbital ordering in the $I4_1/amd$ tetragonal symmetry,⁷ but later x-ray and neutron experiments on single crystals^{9,10} claimed that the $I4_1/a$ space

group was present with antiferro-orbital ordering in which yz and zx orbitals alternate along the c axis. Although $I4_1/a$ space group allows only antiferro-orbital order due to the symmetry consideration, Chung *et al.*¹⁵ pointed out that the large exchange coupling along c determined by neutron scattering is contradictory with the simple antiferro-orbital ordering. In fact, taking into account the staggered trigonal distortion, recent first-principles calculations proposed a orbital ordering in which the same orbital forms “antiferro” orbital order by rotating its direction by $\sim 45^\circ$ alternately within and between orbital chains, while maintaining $I4_1/a$ symmetry.¹⁴ The orbital ordering model reconciles the contradicting experimental results and, indeed, is in good agreement with our nuclear-magnetic resonance (NMR) results. The three proposed orbital ordering models are schematically drawn in Fig. 1.

In order to investigate the orbital and magnetic order microscopically, we have carried out ^{51}V NMR as a function of field (H) and temperature (T) within the FEM state. In zero field, the ^{51}V nuclear spins levels are split by an internal hyperfine field from the ordered Mn and V moments. The field dependence of the resonance reveals the noncollinear nature of the ordered moments. Single ferrimagnetic domain is formed above $H_c \sim 0.3$ T, while the orbital ordering is intact up to 13 T.

^{51}V NMR spectra were obtained on a single crystal of MnV_2O_4 between 4 and 35 K in zero field and in external fields up to 13 T. The preparation of the single crystal of MnV_2O_4 has been described in detail in Ref. 8. The spectra were obtained by integrating averaged spin-echo signals as the frequency was swept through the resonance line. The V resonance in the single crystal (SC) is close to 285 MHz as we found in previous measurement of a polycrystal (PC) sample.¹⁶ However, the spectrum in the SC is narrower than in the PC and reveals two sharp features, whereas the PC sample is significantly broader with poorly resolved features (Fig. 2). These differences are consistent with recent x-ray diffraction and magnetization measurements,⁹ as well as specific-heat data,⁸ which show evidence of an impurity cubic phase resulting from nonstoichiometric crystallites in PC

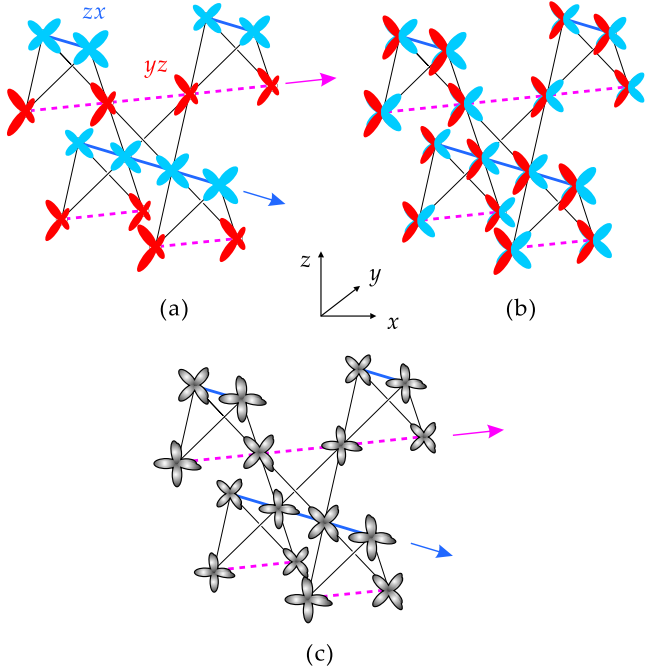


FIG. 1. (Color online) Proposed orbital ordering models: (a) staggered antiferro-orbital order in $I4_1/a$ symmetry (Refs. 9 and 10), (b) ferro-orbital order in $I4_1/amd$ symmetry (Ref. 7), (c) “antiferro”-orbital order in $I4_1/a$ symmetry (Ref. 14). Blue (solid) and red (dotted) lines represent orbital chains running along the edges, corresponding to $[110]$, of the corner-shared V tetrahedra.

samples.⁸ The spectrum of SC clearly shows two narrow lines, but also reveals weak signals, in particular, near 270 and 305 MHz, due to a small portion of the impurity cubic phase remained in SC sample.

In the absence of quadrupolar effects, the V resonance

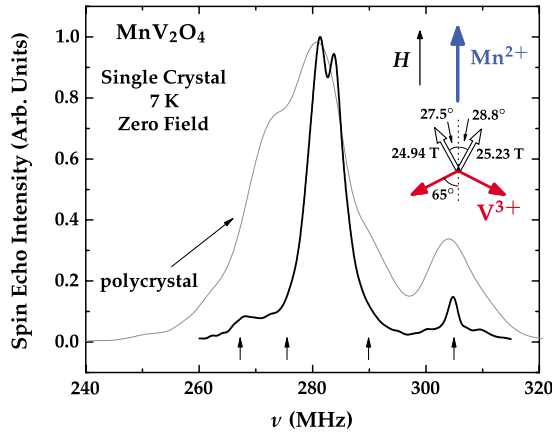


FIG. 2. (Color online) ^{51}V spectrum of single crystal at zero field. Compared with spectrum of polycrystal, the structure is much simple and narrow, indicating that single crystal is relatively free of the impurity cubic phase. The contribution of small impurity phases remaining in the single crystal are indicated by arrows. Two main peaks in single-crystal spectrum implies the existence of inequivalent V sublattices, as depicted in inset, in which hyperfine fields at V nuclei (empty arrows) are not antiparallel to the V^{3+} spin moments. The heights of two spectra were normalized for comparison.

frequency is given by $\nu_0 = \gamma_N H_{\text{hf}}$ where $\gamma_N = 11.195 \text{ MHz/T}$ is the nuclear gyromagnetic ratio, and H_{hf} is the hyperfine field at the V. *A priori*, one might expect that the two well resolved peaks might arise from the second-order quadrupolar contribution in the orbitally ordered state. In this case, the splitting can be written as¹⁷ $\Delta\nu = 25\nu_Q^2/144\nu_0[I(I+1)-3/4]$ and the NQR frequency ν_Q is estimated to be $\sim 40 \text{ MHz}$. Since, however, we are unable to find any satellite transitions associated with the first-order quadrupole splitting, we conclude that ν_Q is negligibly small and the origin of the two peaks is not quadrupolar in nature. Thus the two peaks must arise from two different *hyperfine* fields at different V sublattices which exist only in a state with both long-range orbital and spin order.

It is clear that there is only one V site in the cubic spinel structure above T_S . The proposed $I4_1/a$ tetragonal structure below T_S exhibits a slight contraction of the VO_6 octahedra along the c direction, but still retains a single crystallographic V site.¹⁰ However, the hyperfine fields at V nuclei can be differentiated. The net hyperfine field at the V can be written as the sum of on-site and transferred terms: $\mathbf{H}_{\text{hf}} = \mathbf{H}_{\text{hf}}^{\text{on-site}} + \mathbf{H}_{\text{hf}}^{\text{trans}}$. Each term can be decomposed as:

$$\mathbf{H}_{\text{hf}}^{\text{on-site}} = \mathbf{H}_F + \mathbf{H}_l + \mathbf{H}_d, \quad (1)$$

$$\mathbf{H}_{\text{hf}}^{\text{trans}} = \sum_i A_i \mathbf{S}^i + \sum_j B_j \mathbf{S}_{\text{Mn}}^j, \quad (2)$$

where \mathbf{H}_F is the Fermi contact field arising from the core polarization, \mathbf{H}_l the orbital term from the orbital momentum \mathbf{L} , \mathbf{H}_d the dipolar field from the on-site electrons, the indices i and j are over nearest neighbors V and Mn spin moments, respectively. For an orbital triplet ion, the orbital momentum is only partially quenched¹⁸ and could be as large as $0.34\mu_B$ in MnV_2O_4 ,¹⁴ causing large \mathbf{H}_l and \mathbf{H}_d . On the other hand, the transferred terms are usually very small compared to the on-site term¹⁹ but could be large enough to produce two peaks.

In the case of the perfect antiferro-orbital order^{9–11} or ferro-orbital order,^{7,12} the hyperfine fields should be identical for all of the V sites. Therefore, our data suggest that (i) the tetragonal symmetry is lower than $I4_1/a$ to allow the two V sites, or (ii) the orbital ordering is somewhat complex, yet without lowering the tetragonal symmetry $I4_1/a$. Case (i) is ruled out basing on the neutron and x-ray results^{9,10} so that we assume that case (ii) is applicable. Indeed, case (ii) is realized in the orbital ordering model proposed by Sarkar *et al.*¹⁴ in which the same orbital rotates alternately within and between orbital chains by about 45° . Since the model was obtained by taking into consideration the trigonal distortion of VO_6 octahedra in addition to the tetragonal contraction, it naturally explains the two V sublattices still in the $I4_1/a$ tetragonal symmetry because the V-V and Mn-V transferred hyperfine fields become different for two V sublattices depending on the orbital overlap between V-V and/or V-Mn via oxygen $2p$ orbitals [see Fig. 1(c)].

The two differentiated V sites appear to be robust against the variation of temperature and external field. As shown in Fig. 3, with increasing T , the spectrum shifts to lower frequencies, while retaining the same shape. Since H_{hf} is pro-

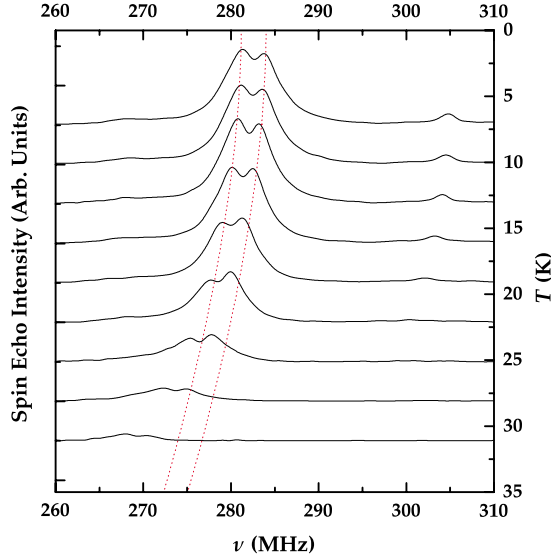


FIG. 3. (Color online) Temperature dependence of ^{51}V spectrum in zero field. A Boltzmann correction by multiplying T was made. The signal becomes weak rapidly with increasing T and disappears above 35 K due to the shortening of T_2 associated with thermal fluctuation. Dotted lines are Eq. (3), implying that the spin-wave theory is applicable at low T region. Seemingly different T dependence of relative intensities between two peaks is ascribed to the impurity cubic phase in which resonance frequencies are almost T independent (Ref. 16).

portional to the sublattice magnetization, we expect $\nu(T)$ to follow Bloch's $T^{3/2}$ law at $T \ll T_N$. If there is an energy gap, E_g , in the spin-wave excitation spectrum, $\nu(T)$ at sufficiently low T is given by

$$\nu(T) = \nu(0)[1 - aT^{3/2}e^{-E_g/T}], \quad (3)$$

where a is a fitting parameter.²⁰ The dotted lines in Fig. 3 are fits to this expression using $E_g = 17.4$ K.¹⁰ The fit is excellent for $T < 15$ K, but deviates above $T \gtrsim 0.25T_N$. Unfortunately, we lose the signal near 30 K due to short spin-spin relaxation rates, $1/T_2$, which increase as thermal fluctuations set in near the phase transition at $T_N = 56$ K.

We now turn to the external field dependence of the spectrum. Figure 4 shows the two peaks as a function of H at 7 K. The initial slope of $\nu(H)$ vs. H is zero as seen in the inset of Fig. 4. With increasing H , the slope increases gradually and reaches a fixed value above $H_c \sim 0.3$ T. This behavior indicates the existence of the FEM domain structure in zero field and its alignment along the external field H , forming a single domain above H_c . This is also consistent with the magnetization M in field that is saturated to $3.2\mu_B$ at H_c , as shown in the inset of Fig. 4. Interestingly, M becomes zero as $H \rightarrow 0$. The absence of the remanent field, despite the “hysteresis” in field, can be understood by assuming the strong coupling between the structural and the magnetic domains. In field, the two domain structures can be decoupled because the directions of the tetragonal domains are limited to three crystallographic axes while the magnetic ones can be aligned in any direction. Therefore, our data suggest that the

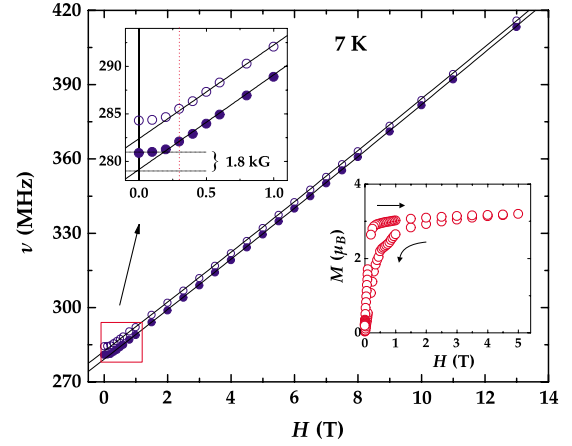


FIG. 4. (Color online) External field dependence of resonance frequencies of two peaks at 7 K. Low field data are enlarged in inset. Zero slope at $H=0$ indicates the existence of domain structure. Excellent fit above 0.3–13 T with Eq. (4) was obtained with the fixed set of parameters (see text), indicating the formation of single domain above 0.3 T, and the robust spin structure up to 13 T. Inset shows the magnetization M in field along the $[110]$ direction at the same T . M is saturated to $3.2\mu_B$ as expected from the non-collinear spin structure.

aligned tetragonal domains⁹ along H become random as $H \rightarrow 0$, and so do the magnetic ones due to the strong coupling between them.

The resonance frequency of the V is given by the net vector sum of the hyperfine and external fields at the nucleus,

$$\nu(H) = \gamma_N |\mathbf{H}_{\text{hf}} + \mathbf{H}| = \gamma_N \sqrt{H_{\text{hf}}^2 + H^2 + 2H_{\text{hf}}H \cos \theta}, \quad (4)$$

where θ is the angle between H_{hf} and H . This equation is plotted in Fig. 4 as a solid line, and clearly fits both peaks up to 13 T with the two parameters H_{hf} and θ for each peak. We find that the fields and angles are 24.94 T with $\theta = 27.5^\circ$ and 25.23 T with $\theta = 28.8^\circ$. Since Mn^{2+} is an orbital singlet ion ($3d^5, L=0$), the Mn^{2+} moment can be easily aligned along H due to its large moment¹⁰ ($4.2\mu_B$) and the essentially isotropic susceptibility. Then the Mn-V and V-V exchange interactions maintain the noncollinear FEM spin structure, which is depicted in the inset of Fig. 2. The excellent fits of data to Eq. (4) indicate that the noncollinear spin structure remains robust up to 13 T. We emphasize that the different angles and hyperfine fields at two V sites are inconsistent with either *simple* antiferro- or ferro-orbital ordering because the V site are equivalent in both cases. Again, however, “antiferro” orbital chains formed by rotating orbitals with respect to each other¹⁴ is compatible with the two inequivalent V sites because the hyperfine fields at ^{51}V nuclei can vary depending on the direction of the orbitals and/or on different overlaps of the on-site orbital with surrounding V d or O $2p$ orbitals.

We note, however, that the angles we obtain ($\sim 28^\circ$) differ significantly from those measured by neutron scattering ($\sim 65^\circ$).^{6,10} This result suggests that either (i) the orientation of the ordered spins changes in field, or (ii) \mathbf{H}_{hf} is not coincident with the direction of the ordered V moments. Case (i) is possible if the delicate balance of exchange fields that

gives rise to the particular FEM structure in zero field is modified by the presence of an external field. However, case (i) seems unlikely because the magnetization data at 7 K shows the saturation moment of about $3.2\mu_B$ (inset of Fig. 4), which is very close to the expected value of $3.1\mu_B$ from the given moments and the angle of $\sim 65^\circ$.¹⁰ Therefore, the large tilted angles of $\sim 35^\circ$ between $-\mathbf{S}$ and \mathbf{H}_{hf} requires that the on-site orbital and dipolar terms be the same order as the isotropic Fermi contact term that is parallel to $-\mathbf{S}$. For the V^{3+} ion, we can estimate the Fermi term $H_F \sim -28$ T.²¹ The anisotropic dipolar term can be estimated from the relation $H_d = 4/7 \langle r^{-3} \rangle \mu_B = 2/7 \times 125 \langle r^{-3} \rangle_{\text{a.u.}}$ kG.²² Using $\langle r^{-3} \rangle_{\text{a.u.}} = 3.217$,¹⁸ $H_d \sim 11.4$ T. For the orbital term, the magnitude of H_l could be approximated as $125 \langle r^{-3} \rangle_{\text{a.u.}} = 40$ T for fully unquenched angular momentum.²¹ Taking into account the quenching, H_l is expected to be the same order as the dipolar term, and is not necessary to be parallel to H_F , resulting in the total hyperfine field that is quite off the direction of the ordered moment. In this sense, the large tilted angle of \mathbf{H}_{hf} could be understood as a consequence of the complex orbital ordering in the orbital triplet ground state of V^{3+} ion, since

the angular momentum is quenched in the perfect antiferro-orbital ordering.⁹

In conclusion, our ^{51}V NMR study on a single crystal of MnV_2O_4 reveals the two inequivalent V sublattices that imply a complicated orbital ordering pattern in the $I4_1/a$ symmetry. Although we cannot determine a specific orbital ordering solely by NMR, our data put a strong constraint on the possible orbital ordering models. We find that the model proposed by Sarkar *et al.*¹⁴ is quite promising being compatible with our data. Also we have shown that the orbital ordering and the noncollinear spin structure are robust up to 13 T.

We thank Hironori Sakai and Stuart E. Brown for useful discussions and suggestions. This work was performed at Los Alamos National Laboratory under the auspices of the U.S. Department of Energy Office of Science. Also this work was supported by NSF in-house research program State of Florida under Cooperative Agreement No. DMR-0084173 and by the EIEG program at FSU.

¹K. I. Kugel' and D. I. Khomskii, Sov. Phys. Usp. **25**, 231 (1982).

²P. G. Radaelli, New J. Phys. **7**, 53 (2005).

³H. Mamiya, M. Onoda, T. Furubayashi, J. Tang, and I. Nakatani, J. Appl. Phys. **81**, 5289 (1997).

⁴Y. Ueda, N. Fujiwara, and H. Yasuoka, J. Phys. Soc. Jpn. **66**, 778 (1997).

⁵M. Onoda and J. Hasegawa, J. Phys.: Condens. Matter **15**, L95 (2003).

⁶R. Plumier and M. Sougi, Physica B **155**, 315 (1989).

⁷K. Adachi, T. Suzuki, K. Kato, K. Osaka, M. Takata, and T. Katsufuji, Phys. Rev. Lett. **95**, 197202 (2005).

⁸H. D. Zhou, J. Lu, and C. R. Wiebe, Phys. Rev. B **76**, 174403 (2007).

⁹T. Suzuki, M. Katsumura, K. Taniguchi, T. Arima, and T. Katsufuji, Phys. Rev. Lett. **98**, 127203 (2007).

¹⁰V. O. Garlea, R. Jin, D. Mandrus, B. Roessli, Q. Huang, M. Miller, A. J. Schultz, and S. E. Nagler, Phys. Rev. Lett. **100**, 066404 (2008).

¹¹H. Tsunetsugu and Y. Motome, Phys. Rev. B **68**, 060405(R) (2003).

¹²O. Tchernyshyov, Phys. Rev. Lett. **93**, 157206 (2004).

¹³S. Di Matteo, G. Jackeli, and N. B. Perkins, Phys. Rev. B **72**, 020408(R) (2005).

¹⁴S. Sarkar, T. Maitra, R. Valentí, and T. Saha-Dasgupta, Phys. Rev. Lett. **102**, 216405 (2009).

¹⁵J.-H. Chung, J.-H. Kim, S.-H. Lee, T. J. Sato, T. Suzuki, M. Katsumura, and T. Katsufuji, Phys. Rev. B **77**, 054412 (2008).

¹⁶S.-H. Baek, K.-Y. Choi, A. P. Reyes, P. L. Kuhns, N. J. Curro, V. Ramachandran, N. S. Dalal, H. D. Zhou, and C. R. Wiebe, J. Phys.: Condens. Matter **20**, 135218 (2008).

¹⁷G. C. Carter, L. H. Bennett, and D. J. Kahan, *Metallic Shift in NMR* (Pergamon, New York, 1977).

¹⁸A. Abragam and B. Bleaney, *Electron Paramagnetic Resonance of Transition Ions* (Clarendon, London, 1970).

¹⁹J. Kikuchi, H. Yasuoka, Y. Kokubo, Y. Ueda, and T. Ohtani, J. Phys. Soc. Jpn. **65**, 2655 (1996).

²⁰A. Narath, in *Hyperfine Interactions*, edited by A. J. Freeman and R. B. Frankel (Academic, New York, 1967).

²¹E. D. Jones, Phys. Rev. **137**, A978 (1965).

²²T. Kubo, A. Hirai, and H. Abe, J. Phys. Soc. Jpn. **26**, 1094 (1969).